

Elastic stability of DNA configurations. II. Supercoiled plasmids with self-contact

Bernard D. Coleman,^{1,*} David Swigon,^{1,†} and Irwin Tobias^{2,‡}

¹*Department of Mechanics and Materials Science Rutgers, The State University of New Jersey, Piscataway, New Jersey 08854*

²*Department of Chemistry, Rutgers, The State University of New Jersey, Piscataway, New Jersey 08854*

(Received 16 July 1999)

Configurations of protein-free DNA miniplasmids are calculated with the effects of impenetrability and self-contact forces taken into account by using exact solutions of Kirchhoff's equations of equilibrium for elastic rods of circular cross section. Bifurcation diagrams are presented as graphs of excess link, $\Delta\mathcal{L}$, versus writhe, \mathcal{W} , and the stability criteria derived in paper I of this series are employed in a search for regions of such diagrams that correspond to configurations that are stable, in the sense that they give local minima to elastic energy. Primary bifurcation branches that originate at circular configurations are composed of configurations with D_m symmetry ($m=2,3,\dots$). Among the results obtained are the following. (i) There are configurations with C_2 symmetry forming secondary bifurcation branches which emerge from the primary branch with $m=3$, and bifurcation of such secondary branches gives rise to tertiary branches of configurations without symmetry. (ii) Whether or not self-contact occurs, a noncircular configuration in the primary branch with $m=2$, called branch α , is stable when for it the derivative $d\Delta\mathcal{L}/d\mathcal{W}$, computed along that branch, is strictly positive. (iii) For configurations not in α , the condition $d\Delta\mathcal{L}/d\mathcal{W}>0$ is not sufficient for stability; in fact, each nonplanar contact-free configuration that is in a branch other than α is unstable. A rule relating the number of points of self-contact and the occurrence of intervals of such contact to the magnitude of $\Delta\mathcal{L}$, which in paper I was found to hold for segments of DNA subject to strong anchoring end conditions, is here observed to hold for computed configurations of protein-free miniplasmids.

PACS number(s): 87.10.+e, 46.70.Hg, 02.40.-k, 46.32.+x

I. INTRODUCTION

In paper I of this series on the theory of the elastic rod model for DNA [1], we derived several criteria for the elastic stability of a calculated equilibrium configuration of a DNA segment that is either a plasmid (i.e., a closed ring) or a linear segment subject to strong anchoring end conditions. We here apply the criteria to a classical problem: analysis of the stability of supercoiled configurations of protein-free plasmids. (See, e.g., Le Bret [2] and Jülicher [3].)

Our results hold for the theory of the commonly employed elastic rod model which treats a DNA segment as an intrinsically straight, homogeneous, inextensible rod with elastic properties that are characterized by two elastic constants, the flexural rigidity A and the torsional rigidity C . Hence, the configuration \mathcal{Z} of a DNA segment is determined once one has specified the curve \mathcal{C} representing the duplex axis and the density $\Delta\Omega$ of the excess twist about \mathcal{C} . The elastic energy Ψ of the segment is the sum of a bending energy Ψ_B which depends on the curvature κ of \mathcal{C} and a twisting energy Ψ_T which depends on $\Delta\Omega$. Thus,

$$\Psi = \Psi_B + \Psi_T, \quad (1)$$

and, when Ψ , Ψ_B , and Ψ_T are expressed in units of A/L with L the length of the segment,

$$\Psi_B = \frac{L}{2} \int_0^L \kappa(s)^2 ds, \quad \Psi_T = \frac{\omega L}{2} \int_0^L \Delta\Omega(s)^2 ds, \quad (2)$$

where

$$\omega = C/A. \quad (3)$$

In earlier studies of the elastic rod model (cf. Refs. [4–6]), explicit (and exact) solutions of Kirchhoff's equations were employed to calculate equilibrium configurations free from points of self-contact. The configurations and bifurcation diagrams shown here and in paper I were calculated using generalizations of those explicit solutions for cases in which excluded volume effects and forces arising from self-contact must be taken into account.

We are concerned with plasmids, i.e., segments for which both DNA strands form closed curves. The excess link in a plasmid, $\Delta\mathcal{L}$, is a topological constant, which, by a now familiar result [7,8], obeys the equation

$$\Delta\mathcal{L} = \mathcal{W} + \Delta\mathcal{T}, \quad (4)$$

in which,

$$\Delta\mathcal{T} = \frac{1}{2\pi} \int_0^L \Delta\Omega ds, \quad (5)$$

and \mathcal{W} is the writhe of the closed curve \mathcal{C} . There are several equivalent definitions of writhe; one, due to Fuller [9], was mentioned in paper I. For a sufficiently smooth curve \mathcal{C} , one may write (see, e.g., the introductory survey [10])

*Electronic address: bcoleman@stokes.rutgers.edu

†Electronic address: swigon@jove.rutgers.edu

‡Electronic address: tobias@rutchem.rutgers.edu

$$\mathcal{W} = \frac{1}{4\pi} \int_0^L \int_0^L \frac{\mathbf{t}(s) \times \mathbf{t}(s^*) \cdot [\mathbf{x}(s) - \mathbf{x}(s^*)]}{|\mathbf{x}(s) - \mathbf{x}(s^*)|^3} ds ds^*, \quad (6)$$

in which $\mathbf{t}(s)$ is the unit tangent vector for \mathcal{C} , and $\mathbf{x}(s)$ is the location in space of the point on \mathcal{C} with arc-length parameter s .

We confine our attention to knot-free plasmids which are modeled as elastic, but impenetrable, closed rods (i.e., rings) for which the cross sections are circular with an invariant diameter D . The two important parameters for the calculations we present are ω and

$$d = D/L. \quad (7)$$

We assume that no external forces act on the plasmid under consideration, and that disjoint subsegments of the plasmid can interact only through contact. We assume further that when such contact occurs, the contact forces are normal to the surfaces of segments involved and moments are not exerted at points of contact; hence changes in configuration do no work against the contact forces.

A configuration is called an *equilibrium configuration* if $\delta\Psi$, the first variation of Ψ , vanishes for each variation $\delta\mathcal{Z}$ in configuration that is *admissible* in the sense that it is compatible with the imposed constraints, which include the requirement that such topological properties as the value of $\Delta\mathcal{L}$ and the knot-free state of \mathcal{C} be preserved.

In the units employed for Eqs. (1) and (2), those equations imply that the resultant moment on the cross section with arc-length parameter s is

$$\mathbf{M}(s) = \mathbf{t} \times \frac{d\mathbf{t}}{ds} + \omega \Delta\Omega \mathbf{t}. \quad (8)$$

In an equilibrium configuration of the plasmid, at values of s other than those characterizing points of self-contact, $\mathbf{M}(s)$ and the resultant force $\mathbf{F}(s)$ obey the equations

$$\frac{d\mathbf{F}}{ds} = \mathbf{0}, \quad \frac{d\mathbf{M}}{ds} = \mathbf{F} \times \mathbf{t}. \quad (9)$$

These two balance equations, with \mathbf{M} as in Eq. (8), yield a system of equations for \mathcal{C} and $\Delta\Omega$ which can be solved in terms of elliptic functions and integrals for a subsegment between points of self-contact (see, e.g., Refs. [4] and [6]). Each such solution is determined by six solution parameters. A plasmid with n points of contact has $2n$ contact-free subsegments, and hence its configuration is determined when $12n$ solution parameters are specified. The condition of pre-assigned $\Delta\mathcal{L}$ and equations rendering precise geometric constraints at contact points and laws of balance of forces and moments at those points (i.e., Eqs. (44) and (45) of paper I) yield $12n$ equations which can be solved to calculate the solution parameters [11]. In this manner we obtain the (constant) value of $\Delta\Omega$ and a precise analytic representation of \mathcal{C} for equilibrium configurations in which self-contact occurs at a finite number of points. The closed form expressions for \mathcal{C} yield formulas that greatly facilitate calculations both of the elastic energy Ψ (cf. Ref. [5]) and of the integral along \mathcal{C} of the geometric torsion (cf. Ref. [6]). Once the torsion integral is known, the writhe \mathcal{W} of \mathcal{C} is determined to within an

integer, called the self-link (cf. Refs. [7] and [12]). In the cases considered here, that integer is not difficult to evaluate (for details see Refs. [6] and [11]).

As in paper I, we here call equilibrium configuration $\mathcal{Z}^\#$ *stable* if it gives a strict local minimum to Ψ in the class of configurations compatible with the constraints. In other words, $\mathcal{Z}^\#$ is stable if and only if it has a neighborhood \mathcal{N} such that $\Psi(\mathcal{Z}) > \Psi(\mathcal{Z}^\#)$ for each configuration \mathcal{Z} in \mathcal{N} that is not equivalent to $\mathcal{Z}^\#$ and is accessible from $\mathcal{Z}^\#$ by a homotopy compatible with the constraints. (Lack of equivalence means that the two configurations, $\mathcal{Z}^\#$ and \mathcal{Z} , differ in distribution of twist density or are such that the corresponding curves, $\mathcal{C}^\#$ and \mathcal{C} , are not congruent, or both.)

As we remarked in paper I, our definition of stability, as it requires that Ψ have a strict *local* minimum, differs from a concept of stability often used in physics (see, e.g., Ref. [3]) which, in the present subject, would require Ψ to have a *global* minimum, i.e., to not exceed its minimum value for any other configuration that may be reached by an arbitrarily large variation compatible with the constraints. A configuration that is *stable* according to our definition but does not give a global minimum to the appropriate energy would be called “metastable” in other contexts.

When a configuration $\mathcal{Z}^\#$ is a member of a one-parameter family E of equilibrium configurations \mathcal{Z} for which one can take $\Delta\mathcal{L}$, $\Delta\mathcal{T}$, and Ψ to be given by functions $\Delta\mathcal{L}^E$, $\Delta\mathcal{T}^E$, and Ψ^E of \mathcal{W} , as in bifurcation diagrams presented here and in paper I, $\mathcal{Z}^\#$ is stable only if the slope of the graph of $\Delta\mathcal{L}$ versus \mathcal{W} for E is not negative at $\mathcal{Z}^\#$. Thus the relation

$$d\Delta\mathcal{L}^E/d\mathcal{W} \geq 0, \quad (10)$$

which we call the *E condition*, is a necessary (but not sufficient) condition for stability. (This condition, derived in paper I under assumptions more general than the present, was obtained in a different form in a seminal paper by Le Bret [2].)

On a cautionary note we mention, as we did in paper I, that there are exceptional families of equilibrium configurations for which $\Delta\mathcal{L}$ is *not* determined by \mathcal{W} , because, for them, equilibrium is maintained when $\Delta\mathcal{L}$ is changed with \mathcal{C} kept constant. Such is the case for those configurations of a plasmid in which \mathcal{C} is a true circle, i.e., the configurations that form the “trivial branch,” which is labeled ζ in the bifurcation diagram shown in Fig. 1 below.

An equilibrium configuration in E for which the excess twist density $\Delta\Omega$ vanishes remains an equilibrium configuration when the plasmid is nicked, i.e., when one of its two DNA strands is severed. In paper I it is shown that a strengthened form of the relation (10), namely,

$$d\Delta\mathcal{L}^E/d\mathcal{W} \geq 1, \quad (11)$$

called the *n condition*, is a necessary condition for an equilibrium configuration in E with $\Delta\Omega = 0$ to be stable both before and after nicking.

In order for an equilibrium configuration $\mathcal{Z}^\#$ to be stable, it is necessary that, for each ξ between 0 and L , there hold $\theta(\xi) \geq 0$, where $\theta(\xi)$ is the slope of the graph of $\Delta\mathcal{L}$ versus \mathcal{W} for the family of equilibrium configurations of the plasmid that contains $\mathcal{Z}^\#$ and is subject to the additional condition that the subsegment with $\xi \leq s \leq L$ be held rigid. [For the

formal definition of $\theta(\xi)$ see Eq. (29) of paper I.] In the present paper we shall show that this condition, which was derived in paper I and there called the θ condition, can furnish a practical method of demonstrating that certain configurations that obey the E condition are in fact unstable.

In order for an equilibrium configuration to be stable it is necessary that the curve \mathcal{C} representing the duplex axis give a strict local minimum to the bending energy Ψ_B in the class of curves that obey constraints and have the same writhe as \mathcal{C} . This \mathcal{W} condition, like the θ condition, can yield a method of further testing the stability of configurations known to obey the E condition.

Arguments given in paper I show that strengthened forms of the E condition and the \mathcal{W} condition can be combined to obtain a condition sufficient for stability, called the S condition, which in the present context may be stated as follows: An equilibrium configuration $\mathcal{Z}^\#$ in E is stable if $d\Delta\mathcal{L}^E/d\mathcal{W} > 0$ at $\mathcal{Z}^\#$ and, in addition, curve $\mathcal{C}(\mathcal{Z}^\#)$ has a neighborhood \mathcal{N} such that for each \mathcal{Z}^* in the family E with writhe \mathcal{W}^* close to $\mathcal{W}^\#$, there holds $\Psi_B(\mathcal{C}) > \Psi_B\mathcal{C}(\mathcal{W}^*)$ for every closed curve \mathcal{C} in \mathcal{N} that has writhe \mathcal{W}^* and is not congruent to $\mathcal{C}(\mathcal{W}^*)$.

In the next section of the paper we present calculated equilibrium configurations for plasmids and applications of the criteria just stated. The configurations and bifurcation diagrams shown were obtained using the generalized method of explicit solution. The basic parameters in our theory are $d = D/L$ and $\omega = C/A$. For the cross-sectional diameter D of DNA we employed 20 Å, and we chose L to be the length of a segment for which the number N of base pairs (bp) is 359 (i.e., $L = 359 \times 3.4$ Å). When ω and the configuration (or, equivalently, the solution parameters) are known, the equations of the theory enable us to calculate Ψ , Ψ_B , and Ψ_T in units of A/L (cf. Eqs. (19)–(20) of Ref. [5], which are easily evaluated expressions for Ψ , Ψ_B , and Ψ_T in terms of solution parameters). To express our reported values of Ψ and Ψ_B in kcal/mol, we needed a value for A ; we chose $A = 2.058 \times 10^{-12}$ erg nm, which corresponds to a persistence length of 500 Å at 298 K (cf. Ref. [13]).

Although we have in hand an easily applied rule for transforming the bifurcation diagram (presented as a graph of $\Delta\mathcal{L}$ versus \mathcal{W}) for one value of ω into the bifurcation diagram for another value of ω [Eq. (40) of paper I], and we do describe the way in which the stability of equilibrium configurations depends on ω , we have chosen to present diagrams with ω set equal to 1.5, a value that corresponds to the very high end of the range of experimental results for C [14,15], because it is only at high values of ω that there are ranges of $\Delta\mathcal{L}$ in which stable nonplanar contact-free configurations occur (cf. Jülicher [3]). The low end of the range of experimental determinations of C yields 0.7 for ω [16,17]. Section II concludes with a figure showing how the class of stable configurations for $\omega = 1.5$ differs from that for $\omega = 0.7$.

Here, as in paper I, our calculations are intended to illustrate a method of investigating the elastic stability of configurations, not to argue that specific values of ω or D are appropriate for the ratio of the elastic moduli or the effective diameter of DNA.

The results we present in Sec. II have been obtained with rigor and precision in the theory under consideration, namely that in which a DNA segment is modeled as a homogeneous

rod obeying the special case of Kirchhoff's constitutive relations in which the rod is assumed to be not only both inextensible and kinematically symmetric, but also of circular cross section. Without dwelling on the obvious limitations of such a model as a representation of a true DNA segment, we should like to make two cautionary remarks about the applicability of our results that touch on matters other than the lack of homogeneity and axial symmetry in actual DNA segments:

(i) Since the value of N employed in our calculations corresponds to approximately 2.5 persistence lengths under normal experimental conditions, we do not claim that the configurations we calculate would be free from fluctuations, or that for them one can set differences in Ψ equal to differences in the free energy of supercoiling. (For calculations of the free energy of supercoiling for miniplasmids see, e.g., Refs. [18–22].)

(ii) The calculations we report do not account for the effects of electrostatic repulsion. To do so in an approximate way, one may consider replacing the (average) “geometric” value of D by an “effective” value, say Df , with $f > 1$ (see, e.g., Refs. [23] and [24]). When electrostatic effects are absent, calculations of the type we have performed for plasmids of size N and (geometric) cross-sectional diameter D are applicable to plasmids of size Nf with diameter Df . Equilibrium configurations for specified values of $\Delta\mathcal{L}$ remain essentially the same under such rescaling; i.e., curve \mathcal{C} undergoes a similarity transformation with scale factor f , the excess twist $\Delta\mathcal{T}$ (as well as the writhe \mathcal{W}) remains invariant, and the elastic energy Ψ (in units of kcal/mole) changes to $\Psi^f = \Psi/f$. One may hope that if one chooses f judiciously, one can obtain, from calculations that ignore electrostatic forces, useful, albeit approximate, values of properties of a miniplasmid of size Nf and geometric diameter D that is subject to electrostatic effects.

In Appendix A we discuss an illustrative example which shows that, once one is able to find all the equilibrium configurations in a given region of the $(\Delta\mathcal{L}, \mathcal{W})$ plane, or, equivalently, in the $(\Psi, \Delta\mathcal{L})$ plane, one can find lower bounds for energy barriers for the various pathways by which a transition at fixed $\Delta\mathcal{L}$ from one (locally) stable state to another stable state can be realized. We remark there that before the estimate of activation energy which that example yields can be accepted with confidence, it will be necessary to resolve an open problem mentioned in the last paragraph of Sec. II.

II. CONFIGURATIONS AND BIFURCATION DIAGRAMS

For each pair $(N, \Delta\mathcal{L})$, a plasmid has at least one, and usually several, equilibrium configurations (see, e.g., Refs. [2] and [3]). As $\Delta\mathcal{L}$ varies at fixed N , these configurations vary and form families of equilibrium configurations. We focus our attention on groups of such families, also called *branches*, that contain configurations with three or fewer points of maximum curvature and that are connected to a branch, called the *trivial branch*, which is made up of the configurations for which \mathcal{C} is a circle. In the figures that trivial branch is labeled ζ and is shown as a dotted line. Branches α and β , which originate at a bifurcation point of the trivial branch, are shown as heavy solid lines and are

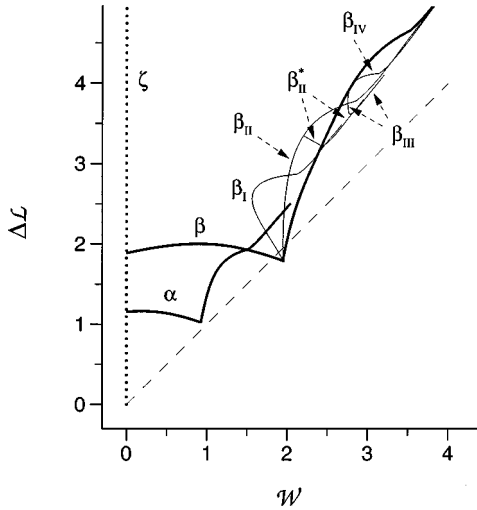


FIG. 1. Bifurcation diagram for a protein-free DNA plasmid with $N=359$ and $\omega=1.5$ drawn as a plot of $\Delta\mathcal{L}$ versus \mathcal{W} . Shown as a dotted (vertical) line is the trivial branch ζ ; two branches, α and β , resulting from bifurcation of ζ are shown as heavy solid curves; four branches, β_1 , β_2 , β_3 , and β_4 , arising from secondary bifurcations of β , and one tertiary branch β_2^* emerging from β_2 , are shown as light solid curves.

called *primary bifurcation branches*. Branches that originate at bifurcation points of a primary branch (and hence are connected to ζ by a single primary branch) are called *secondary bifurcation branches*. In the figures the secondary branches have labels that bear subscripts, e.g., β_1 , β_2, \dots , and are shown as light solid curves. A *tertiary bifurcation branch*, β_2^* , that originates at a bifurcation point of the secondary branch β_2 is also shown as a light solid line (see Fig. 1).

Since the (protein-free and knot-free) plasmids we consider have a symmetry such that for equilibrium configuration the transformation $\Delta\mathcal{L} \rightarrow -\Delta\mathcal{L}$ takes \mathcal{W} into $-\mathcal{W}$ and leaves Ψ unchanged, we take $\Delta\mathcal{L}$ to be positive.

When $\Delta\mathcal{L}$ is less than a critical value, $\Delta\mathcal{L}^*$, a miniplasmid has just one equilibrium configuration and it belongs to ζ . In the present case ($N=359$, $\omega=1.5$), $\Delta\mathcal{L}^*=1.029$ and there are two equilibrium configurations with $\Delta\mathcal{L}=\Delta\mathcal{L}^*$: one is in ζ , and the other, with $\mathcal{W}^*=0.927$, has a single point of self-contact and corresponds to the point A^1 on branch α .

Each point of ζ for which

$$\Delta\mathcal{L} = \omega^{-1} \sqrt{m^2 - 1}, \quad m=2,3,4, \dots, \quad (12)$$

is a bifurcation point at which a family of solutions with $\mathcal{W} \neq 0$ intersects ζ , i.e., at which a primary branch originates [25]. We call the integer m in Eq. (12) the *index* of the primary branch. The first such bifurcation of ζ occurs at $\Delta\mathcal{L} = \Delta\mathcal{L}^\alpha = \omega^{-1} \sqrt{3}$ and gives rise to branch α which has an index of 2; the second occurs at $\Delta\mathcal{L} = \Delta\mathcal{L}^\beta = \omega^{-1} 2\sqrt{2}$ and gives rise to the branch β which has an index of 3. We note that $\Delta\mathcal{L}^*$ is the smaller of the two numbers $\Delta\mathcal{L}^\alpha$ and $\Delta\mathcal{L}(A^1)$, where A^1 is the configuration of minimum writhe which (i) lies in the branch α and (ii) is such that the plasmid has a point of self-contact.

A list of possible symmetry groups of contact-free equilibrium configurations of closed elastic rods with $\Delta\mathcal{L} \neq 0$ was given by Domokos [26]. (His analysis rests on the assump-

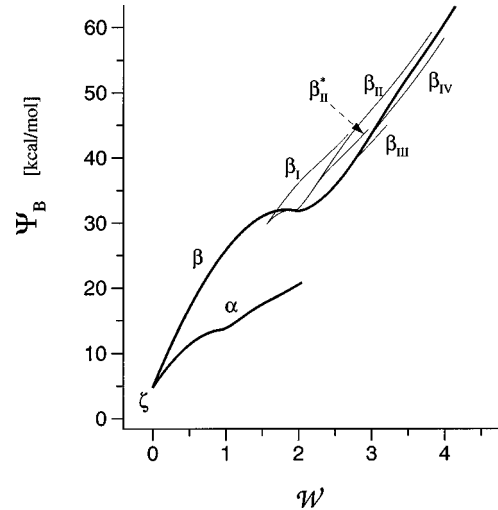


FIG. 2. Graphs of bending energy Ψ_B versus \mathcal{W} for branches of the bifurcation diagram of Fig. 1.

tion that the force vector \mathbf{F} is independent of s , an assumption valid when self-contact does not occur.) We find that for each $m \geq 2$, the symmetry group of all configurations in the primary branch with index m is the dihedral group D_m of order $2m$. Hence, whether or not self-contact is present, the curve \mathcal{C} for a configuration on the primary branch of index m has a single m -fold symmetry axis that is perpendicular to the plane \mathcal{P} containing the $2m$ points at which the curvature κ of \mathcal{C} has a local extremum (i.e., a maximum or a minimum). Each of the m lines that intersect the m -fold symmetry axis and pass through two extrema of κ is a twofold symmetry axis.

It is clear that on the trivial branch ζ there holds $d\mathcal{W}/d\Delta\mathcal{L}=0$, and $\Delta\mathcal{L}$, $\Delta\mathcal{T}$, and Ψ are not given by functions of \mathcal{W} . Although the theory of the E condition and θ condition is not directly applicable to configurations in ζ , one can show that those circular configurations are stable when $\Delta\mathcal{L}$ is less than $\Delta\mathcal{L}^\alpha$, and unstable when $\Delta\mathcal{L}$ is greater than $\Delta\mathcal{L}^\alpha$. (A formal proof of this assertion is given in Appendix B.)

In Fig. 2 we give graphs of Ψ_B versus \mathcal{W} for the branches of the bifurcation diagram of Fig. 1. The utility of such graphs for investigation of the stability of calculated equilibrium configurations of plasmids was noted by Le Bret [2]. Arguments given in paper I imply that here, on each non-trivial branch,

$$d\Psi_B^E/d\mathcal{W} = 4\pi^2\omega\Delta\mathcal{T}^E. \quad (13)$$

This relation, which follows from Eq. (20) of paper I with $P=0$ [see also Ref. [9], Eq. (5)], tells us that the data in Fig. 2 determine $\Delta\mathcal{L}$ as a function, $\Delta\mathcal{L}^E$, of \mathcal{W} , i.e., Fig. 1 can be reconstructed from Fig. 2.

As the configurations in ζ have zero writhe and bending energy $2\pi^2$ (in units of A/L), the trivial branch reduces to a single point in Fig. 2. It follows from Eqs. (12) and (13) that the primary bifurcation branches correspond to curves in Fig. 2 with initial slopes given by

$$\left. \frac{d\Psi_B^E}{d\mathcal{W}} \right|_{\mathcal{W}=0} = 4\pi^2 \sqrt{m^2 - 1}. \quad (14)$$

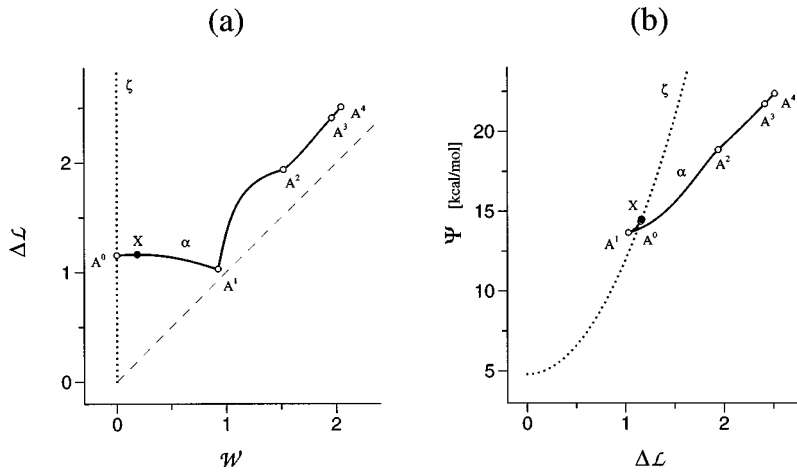


FIG. 3. Graphs of $\Delta\mathcal{L}$ versus \mathcal{W} , and Ψ versus $\Delta\mathcal{L}$, for branches ζ and α . The configurations corresponding to points \circ and \bullet are shown in Fig. 4.

A configuration that minimizes Ψ_B in the class of *equilibrium* configurations with a given writhe also minimizes Ψ_B in the class of *all* configurations with the same writhe. Hence, the calculations that gave us Fig. 2 tell us that for each writhe the global minimum of Ψ_B at that writhe is attained by a configuration in branch α .

Details of the graph of $\Delta\mathcal{L}$ versus \mathcal{W} for branch α are shown in Fig. 3(a). For $n=0, 1, 2,$ and 3 , the configurations with n points of self-contact correspond to points on that graph between A^n and A^{n+1} and form smooth families of equilibrium configurations. As we know that the branch α is a locus of configurations that minimize Ψ_B at fixed \mathcal{W} , we can apply the S condition and assert that a configuration in α is stable if (and only if) it obeys the E condition. Although $d\Delta\mathcal{L}/d\mathcal{W}$ suffers a jump at the points A^n , in the present case the right-hand and left-hand derivatives are positive at A^2 and A^3 , and hence the configurations corresponding to those points are stable. At A^1 , $d\Delta\mathcal{L}/d\mathcal{W}$ has left- and right-hand derivatives that have opposite signs; at the point X, shown as a solid circle in Fig. 2, the derivative $d\Delta\mathcal{L}/d\mathcal{W}$ is continuous

but changes sign. As the branch traverses the points A^1 and X, the corresponding configurations either gain or lose stability; such points are called *points of exchange of stability*. Since, in the present case, $\Delta\mathcal{L}$ is a (strictly) increasing function of \mathcal{W} between A^0 and X, and between A^1 and A^4 , but is a decreasing function between X and A^1 , the configurations in α with \mathcal{W} either between its values at A^0 and X, or between its values at A^1 and A^4 are stable, and those with \mathcal{W} between its values at X and A^1 are unstable.

The configuration A^0 (at which α branches off from ζ), the configuration X (which lies in α between the circular configuration A^0 and the “figure 8” configuration A^1 and which has $d\Delta\mathcal{L}/d\mathcal{W}=0$), and the configurations A^1, \dots, A^4 are shown in Fig. 4. Each of these configurations has D_2 symmetry, i.e., has three twofold symmetry axes, two of which lie in the plane \mathcal{P} . As $\Delta\mathcal{L}$ increases, the number of self-contact points in a configuration on the branch α increases in the sequence 1, 2, 3, until $\Delta\mathcal{L}$ attains its value at A^4 . (For the values of ω and D/L employed here, that value of $\Delta\mathcal{L}$ is 2.521.) A configuration with $\Delta\mathcal{L}$ near to, but greater

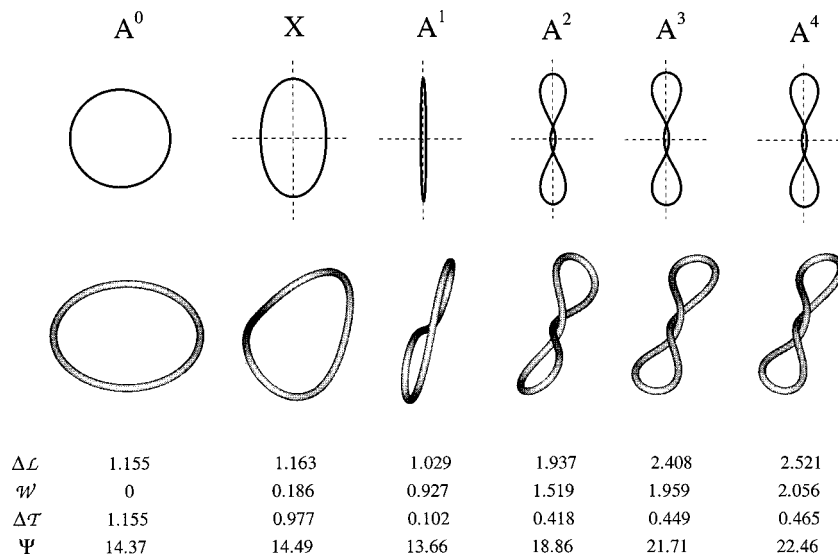


FIG. 4. As explained in the text, configurations at X and A^1 are points of exchange of stability, and for each n , A^n is the configuration of smallest writhe in branch α with n points of self-contact. Here, as in Figs. 6, 8, 9, and 11, the following conventions are employed: the top row shows the projection of \mathcal{C} on plane \mathcal{P} with the twofold symmetry axes in \mathcal{P} , drawn as dashed lines. The bottom row shows the plasmid depicted as a tube of diameter 20 \AA viewed at an angle of 75° to \mathcal{T} . The scale is constant in each row, but is reduced in the top row. Ψ is given in kcal/mol.

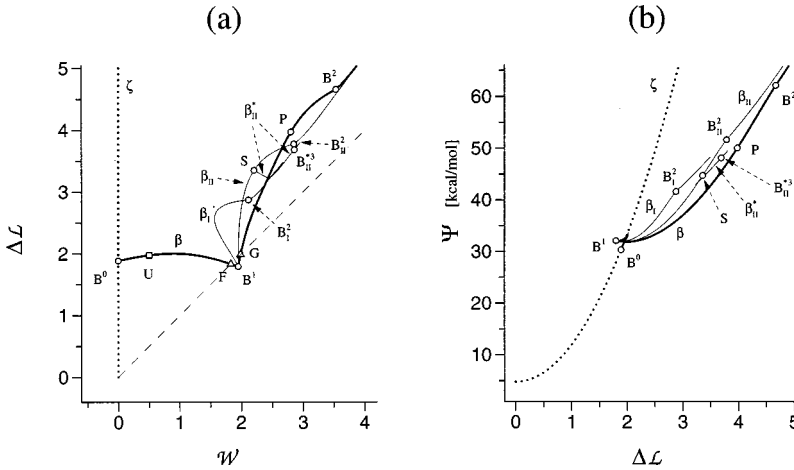


FIG. 5. Graphs of $\Delta\mathcal{L}$ versus \mathcal{W} and Ψ versus $\Delta\mathcal{L}$ for branches ζ , β , β_1 , β_{II} , and β_{II}^* . The configurations corresponding to points \circ , \triangle , and \square are shown in Figs. 6, 8, and 9. Branch β is shown as a heavy solid curve (with kinks at B^1 and B^2) and branches β_1 , β_{II} , and β_{II}^* as light curves (with kinks at B_1^2 and B_{II}^2).

than, 2.521 has two isolated points and an interval of self-contact; for such a configuration, κ attains its minimum at the two values of s corresponding to the midpoint of the interval of self-contact.

The value of \mathcal{W} corresponding to point X is sensitive to ω . Had we here put $\omega=1.4$, as we did in a discussion of mononucleosomes in paper I, the interval between A^0 and X would have been too small to show clearly in Figs. 3(a) and 3(b). Recent calculations discussed below show that when $\omega=1.375$ (i.e., when $\omega=\frac{11}{8}$), $d\Delta\mathcal{L}/d\mathcal{W}=0$ at point A^0 on branch α , and hence points A^0 and X then coincide. Thus, all of the nonplanar contact-free configurations on branch α are unstable if $\omega\leq 1.375$. In addition, we have found that when $\omega=1.993$, points X and A^1 coincide, which implies that all the configurations on branch α are stable if $\omega>1.993$. Because configurations A^0 and X do not show self-contact, but the configuration A^1 does, the value of ω for which X and A^0 coincide is independent of the plasmid size and cross-sectional diameter D , but the value of ω at which X and A^1 coincide depends on the ratio $d=D/L$.

With the exception of Ref. [2], the literature on bifurcation branches in the theory of the elastic rod model for protein-free plasmids deals primarily with branch α . Some relevant recent papers are those of Jülicher [3], Yang *et al.* [27], and Westcott *et al.* [28]. Jülicher [3] modeled a plasmid as an impenetrable rod with zero cross-sectional diameter and considered a configuration stable only if it gives a global minimum to Ψ at fixed $\Delta\mathcal{L}$. If one identifies the configurations that Jülicher refers to as “interwound” with those in α that show two or more points of self-contact, and takes into account differences in assumptions about the diameter of cross-sections, then his $(\omega, \Delta\mathcal{L})$ -phase diagram and observations about the dependence on \mathcal{W} of Ψ_B for configurations in α become compatible with the results shown here in Figs. 2, 3(b), and 12. Yang *et al.* [27] and Westcott *et al.* [28] present not stability analyses but numerical calculations. Yang *et al.* [27] developed a finite element method in which self-contact is taken into account by introducing a penalty function. Westcott *et al.* [28] employed a finite difference method and accounted for the excluded-volume effect that arises from a Debye-Hückel-type electrostatic repulsion. Each of the cited papers contains examples of calculated configurations with evident D_2 symmetry.

There are ranges of ω (with upper bounds depending on d) for which there are values of $\Delta\mathcal{L}$ where either (i) both

branch ζ and branch α contain stable equilibrium configurations with the same $\Delta\mathcal{L}$, or (ii) branch α contains two such stable configurations. The values of ω , N , and D which yield Fig. 3 are such that both (i) and (ii) can occur (for separate ranges of $\Delta\mathcal{L}$). We have found that for the present value of d , (i) occurs when $\omega<1.707$ and $\Delta\mathcal{L}(A^1)<\Delta\mathcal{L}\leq\Delta\mathcal{L}(A^0)=\Delta\mathcal{L}^\alpha$, and (ii) occurs when $1.375<\omega<1.993$ and $\max[\Delta\mathcal{L}(A^1), \Delta\mathcal{L}^\alpha]<\Delta\mathcal{L}<\Delta\mathcal{L}(X)$. When $\omega>1.993$, for each $\Delta\mathcal{L}$ there is precisely one stable equilibrium configuration in the union of branches ζ and α .

Perhaps of greater importance than the observations just made, at least for those concerned with topoisomer distributions, is the fact that there is a range of ω (which is $\omega<1.600$ for the present value of d) such that for a small interval of values of $\Delta\mathcal{L}$ bounded above by $\Delta\mathcal{L}^\alpha$ there are not only two stable configurations, one in α with a single point of self-contact, i.e., a “figure 8,” and the other in ζ , but, in addition, the “figure 8” configuration has lower elastic energy than the circular configuration. (See also Le Bret [2], Tsuru and Wadati [29], and Jülicher [3].)

The graph of $\Delta\mathcal{L}$ versus \mathcal{W} for β , which branches off from ζ at B^0 and has index 3, is shown in Figs. 1 and 5(a). The configurations in β have D_3 symmetry. Those between B^0 and B^1 are contact-free, those between B^1 and B^2 have three points of self-contact, and those with $\Delta\mathcal{L}$ greater than but close to its value (4.653) at B^2 have six points of self-contact. (See Fig. 6.)

For each branch that bifurcates from ζ (including branch β) there is an interval of values of \mathcal{W} containing $\mathcal{W}=0$ for which the corresponding equilibrium configurations are contact-free. (In fact, all nontrivial contact-free configurations are in primary bifurcation branches.) We have found that the contact-free equilibrium configurations in primary branches with index $m>2$ do not obey the θ condition and hence cannot be stable, even if they obey the E condition. (See, for example, the graph of $\theta(\xi)$ versus ξ/L shown in Fig. 7 for the configuration U , which does obey the E condition.) It follows that a protein-free plasmid can have nonplanar stable equilibrium configurations that are contact-free only if $\omega>1.375$, and if such configurations occur, they must be in α . This conclusion is stronger than a result of Le Bret [2] to the effect that for such a plasmid to have stable, nonplanar, contact-free configurations it is necessary that $\omega>1$.

Let ω_m be the value of ω for which the branch that bifurcates from ζ with index m is such that $d\Delta\mathcal{L}/d\mathcal{W}=0$, at the

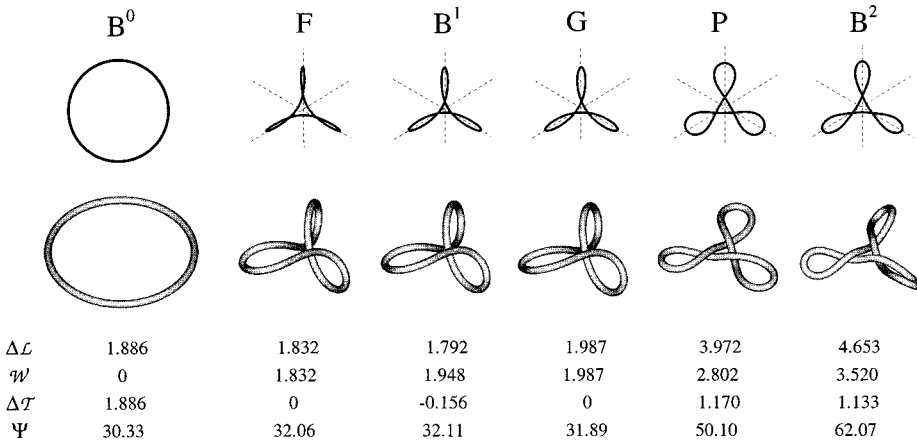


FIG. 6. Selected configurations in the branch β . B^n denotes the configuration of smallest writhe in β with $3n$ points of self-contact. Shown are B^0 , B^1 , and B^2 . The configurations at points F and G would remain in equilibrium if the plasmid were nicked; F is unstable; G is stable and would remain so after nicking. P is the configuration at the point of secondary bifurcation.

point where $\mathcal{W}=0$. If $\omega > \omega_m$, then there are contact-free configurations in the branch with index m obeying the E condition, but if $\omega < \omega_m$ there are no such contact-free configurations in the branch. Applying the explicit solution method for contact-free equilibrium solutions [4–6] to an analysis of solutions near to the circular solutions with ΔL_k as in Eq. (12), we have found that, to within eight significant figures for ω_m ,

$$\omega_m - 1 = 3/(2m^2). \quad (15)$$

In particular, $\omega_2 = \frac{11}{8}$ and, as stated above, if $\omega > \frac{11}{8}$, the interval of points in α corresponding to stable equilibrium configurations is not empty. (For $m > 2$, if $\omega > \omega_m$, the branch with index m will have an interval with contact-free equilibrium configurations that obey the E condition, but, as we have noted, are unstable.)

Since the value of ω that we are using exceeds $\omega_3 = \frac{7}{6}$, there is an interval of writhe values, which in the present case is $0 < \mathcal{W} < 0.900$, for which the configurations in β are contact-free and have $d\Delta\mathcal{L}/d\mathcal{W} > 0$. For $0.900 < \mathcal{W} < 1.948$ (where 1.948 is the writhe of B^1), $d\Delta\mathcal{L}/d\mathcal{W} < 0$. Because all the contact-free configurations in β are unstable, the point in β where $\mathcal{W}=0.900$ is *not* a point of exchange of stability.

We have remarked that the contact-free configurations in β fail to obey the θ condition. One also can show that those configurations do not obey the \mathcal{W} condition by constructing admissible variations with $\delta\mathcal{W}=0$ that lower Ψ_B . Consider, for example, the configuration labeled U in Fig. 5 which has

$\mathcal{W}=0.5$, $\Delta\mathcal{L}=1.975$, and is shown in Fig. 8, where q_0 denotes the distance (32.8 nm) between the two points of extrema of curvature of \mathcal{C} that lie on the twofold axes of symmetry for U. We have constructed a one-parameter set H of configurations $U^{(\eta)}$ of the plasmid such that each configuration in H yields $\delta\Psi=0$ for each variation in \mathcal{C} obeying the constraints that (i) \mathcal{C} has a twofold axis of symmetry, (ii) \mathcal{W} stays at its value in the configuration U, (iii) the distance between the points on the symmetry axis is $q=(1-\eta)q_0$. The members of H with $\eta=0.05, 0.2$, and 0.668 are shown in the figure. Clearly, U is in H with $\eta=0$, and the variation $(\delta\mathcal{Z})_\eta$ that takes U into $U^{(\eta)}$ has $\delta\mathcal{W}=0$. In the present case, $\Psi_B(U^{(\eta)}) < \Psi_B(U)$ for each $\eta \neq 0$, no matter how small. The configuration U^* (corresponding to $\eta=0.668$) is an equilibrium configuration of the plasmid and it lies in branch α .

We now turn to the configurations in β with self-contact. Such configurations have loops. For rods and ropes the concept of a loop is intuitive. DNA segments, such as the subsegment \mathcal{D}^f of a miniplasmid in a mononucleosome (cf. paper I), that are subject to constraints that keep endpoints in proximity are often called loops, even if free from self-contact. Here, when we call a subsegment of a protein-free plasmid a loop, we presuppose that its ends are in contact. At sufficiently large values of the writhe, a loop shows self-contact not only at its end points, but also in its interior. It is in agreement with current usage to call a loop with more than one self-contact a *plectonemic loop*, or, for short, a *plectoneme*.

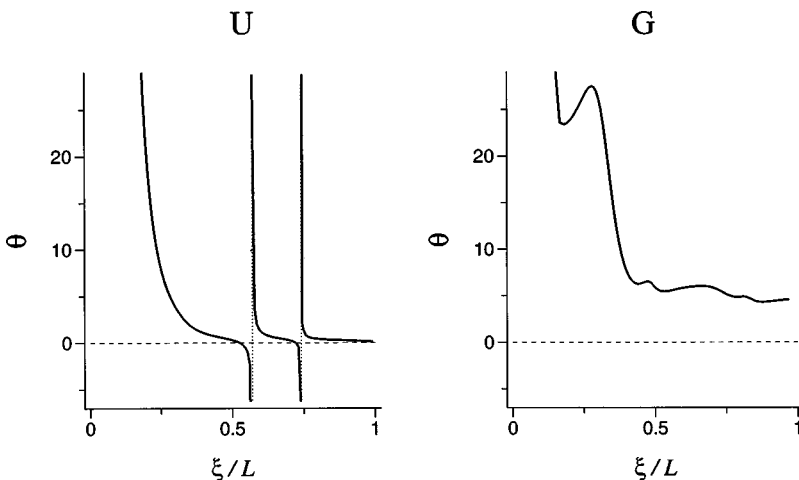


FIG. 7. Graphs of θ versus ξ/L for configurations U and G in branch β that, as seen in Fig. 5, obey the E condition with $d\Delta\mathcal{L}/d\mathcal{W}$ strictly positive. The plasmid is contact-free in configuration U and has three points of self-contact in G. In both cases, $\theta \rightarrow \infty$ as $\xi \rightarrow 0^+$. For G, $\theta(\xi) > 0$ for all $0 \leq \xi < L$; for U, $\theta(\xi)$ vanishes at two values of ξ , and there are two singular values of ξ (marked with vertical dotted lines) at which $\theta \rightarrow +\infty$ from the left and $-\infty$ from the right.

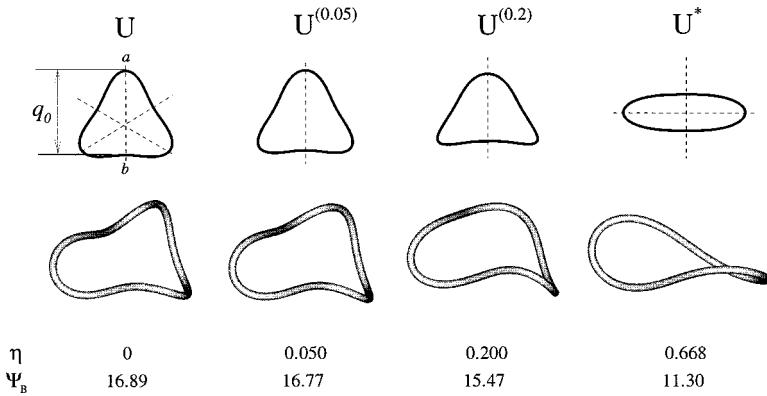


FIG. 8. The configurations $U^{(\eta)}$ are the result of special deformations of U (described in the text) that change the distance between points a and b from q_0 to $(1 - \eta)q_0$ while keeping \mathcal{W} fixed. It turns out that this one-parameter set of deformations lowers Ψ_B .

When $\Delta\mathcal{L}$ exceeds its value at B^1 , the configurations in the branch β have three congruent loops. Between B^1 and B^2 , each such loop has one point of self-contact (at its endpoints). For \mathcal{W} (or, equivalently, for $\Delta\mathcal{L}$) greater than its value at B^2 , these loops are plectonemes.

Points B^1 and P are points of secondary bifurcation. At B^1 , the point on β with the smallest $\Delta\mathcal{L}$ for which self-contact occurs, branches β_I and β_{II} originate. Two other branches, β_{III} and β_{IV} , originate at P . Although, as we have remarked, the configurations in β have (in accord with the known properties of primary branches) one threefold symmetry axis and three twofold symmetry axes, those in β_I – β_{IV} have a symmetry corresponding to group C_2 of order 2, i.e., have only a single twofold symmetry axis and it is unique. (See Figs. 9 and 11.) The configurations in β_I have one loop which, as $\Delta\mathcal{L}$ increases above its value at B^1 , becomes plectonemic. The configurations in β_{II} have two such loops, which are congruent. The configurations in β_{III} and β_{IV} have three loops, of which one intersects the symmetry axis and the other two are congruent. In β_{III} , the loop that intersects the symmetry axis becomes plectonemic when \mathcal{W} increases above its value at B^2_{III} . In β_{IV} , the two congruent loops become plectonemic when \mathcal{W} increases above its value at B^2_{IV} . In each case that we have studied, the number of self-contacts in a plectonemic loop increases in the sequence 1, 2, 3, with an interval of points of self-contact occurring at higher $\Delta\mathcal{L}$. (Such is the case also for the extranucleosomal loop of miniplasmids in mononucleosomes (see paper I) and for plectonemic loops in linear DNA segments subject to tension and torsional moments [11].)

When we say that β_I , β_{II} , β_{III} , and β_{IV} “originate” at a secondary bifurcation point, i.e., are “secondary branches” that “branch off” from the primary branch β , we employ a terminology that follows a natural convention: if, as a parameter (e.g., $\Delta\mathcal{L}$ or \mathcal{W}) is varied, a primary branch enters a point and several other branches exit from the point with precisely one of the exiting branches having the symmetry properties of the primary branch, we consider the branch that exits with the original symmetry to be the continuation of the primary branch and the others to be secondary branches that originate at the bifurcation point.

The notation we used in Figs. 5–11 when we labeled points B^0 , B^1 , B^2 , B^2_1 , etc., has the following property: The configurations in each branch β_a (where β_a stands for β , β_I , β_{II} , β_{III} , β_{IV}) that show at least one loop with p self-contacts, but no loop with $p + 1$ contacts, correspond to the

points in β_a between B^p_a and B^{p+1}_a . In this notation, points B^1_I and B^1_{II} are the same as point B^1 and hence are labeled B^1 , and points B^1_{III} and B^1_{IV} are the same as point P .

The secondary branch β_{II} has a bifurcation point S , at which a tertiary branch, β^*_{II} , originates. The configurations in β^*_{II} have no discernible symmetry; each contains two non-congruent loops. As \mathcal{W} increases, one loop becomes plectonemic, while the other appears to “flatten” (or “become more planar”) as well as “tighten” (or increase in bending energy) (see Fig. 9).

As shown in Fig. 5(a), the graphs of $\Delta\mathcal{L}$ versus \mathcal{W} for branches β , β_I , β_{II} cross the line $\Delta\mathcal{L} = \mathcal{W}$. The configura-

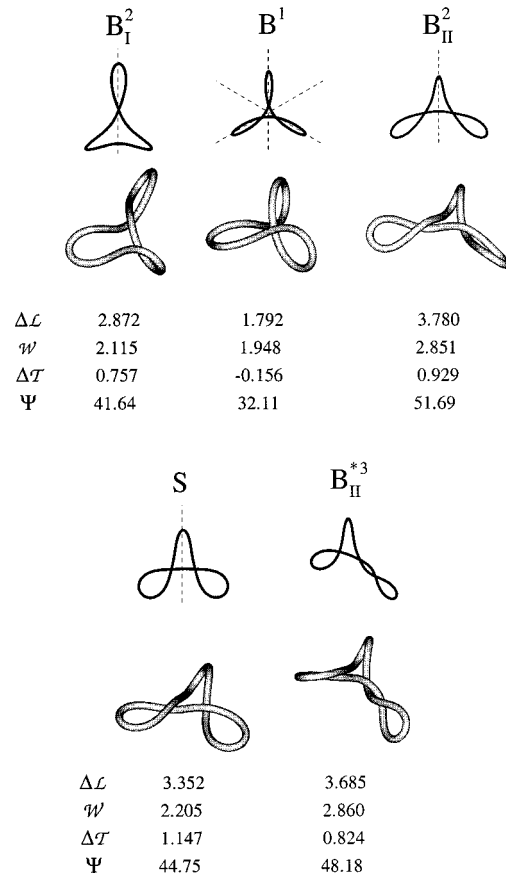


FIG. 9. Shown here are: B^2_I , the configuration of smallest writhe in β_I with two points of self-contact; B^2_{II} , the configuration of smallest writhe in β_{II} with four points of self-contact; S , the configuration at the point of tertiary bifurcation of β_{II} ; and B^*3_{II} , the configuration of smallest writhe in β^*_{II} with four points of self-contact.

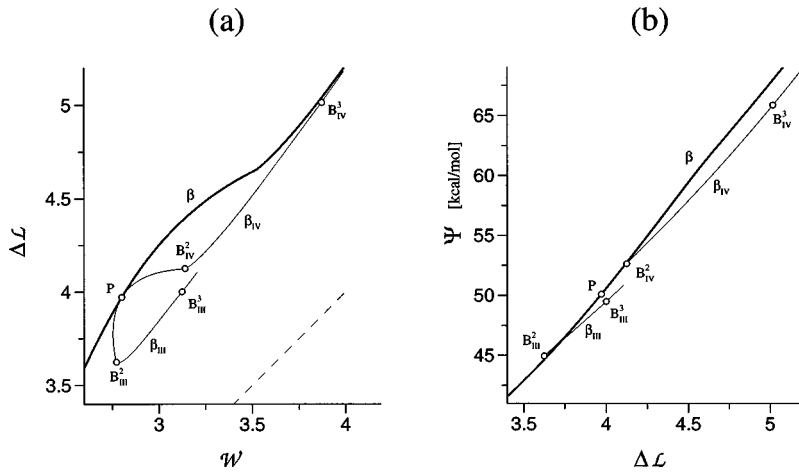


FIG. 10. Graphs of $\Delta\mathcal{L}$ versus \mathcal{W} , and Ψ versus $\Delta\mathcal{L}$, for branches β , β_{III} , and β_{IV} . The configurations corresponding to points \circ are shown in Fig. 11.

tions corresponding to those crossing points would remain in equilibrium if the plasmid were nicked. Such points on branch β are labeled F and G and marked \triangle in Fig. 5(a). At F, $d\Delta\mathcal{L}/d\mathcal{W} < 1$, and hence the corresponding configuration is unstable. Since point G lies between B^1 and P, the configuration corresponding to G obeys the θ condition (see Fig. 7) and, since it obeys the condition $d\Delta\mathcal{L}/d\mathcal{W} > 1$, if it is stable, it will remain so when the plasmid is nicked.

Analysis of the stability of configurations in branches β , $\beta_I - \beta_{IV}$, and β_{II}^* requires care. By using the θ condition, we can show that not only the contact-free configurations in β but also all the configurations (with self-contact points) that are in β_I , β_{II} , or β_{II}^* , or are in β with \mathcal{W} greater than its value at P, or in β_{III} between P and B_{III}^2 , or in β_{IV} between P and B_{IV}^2 are unstable, whether or not they obey the E condition. The remaining configurations, namely those in β between B^1 and P, those in β_{III} with \mathcal{W} greater than $\mathcal{W}(B_{III}^2)$, and those in β_{IV} with \mathcal{W} greater than $\mathcal{W}(B_{IV}^2)$, obey the θ condition. Verification that the S condition holds suffices to prove stability, but such verification usually is not easy, because for equilibrium configurations other than those on the branch α it is a very difficult matter to prove that Ψ_B has a (local) minimum at fixed \mathcal{W} .

Our experience indicates that whenever an equilibrium configuration $Z^\#$ of a plasmid fails to obey the θ condition, we can find a counterexample showing that $Z^\#$ does not give a strict (local) minimum to Ψ_B at fixed \mathcal{W} (see, e.g., Fig. 8). As we have not been able to find such counterexamples for

configurations that do obey the θ condition, we conjecture, with as yet no formal proof, that satisfaction of the θ condition is not only necessary, but also sufficient for stability of an equilibrium configuration of a plasmid. Consequences of this conjecture of sufficiency of the θ condition for stability of configurations of plasmids will be studied in Appendix A. We consider the development of methods of proving or disproving the validity of the conjecture to be a major open problem in our subject. To give some idea of the importance of the problem, we remark that, if the conjecture is correct, then configurations corresponding to points of the heavy solid curves in Fig. 12 are stable (in the sense that they give to Ψ strict local minima in the class of configurations with equal $\Delta\mathcal{L}$), but, until the validity of the conjecture is established, we can assert with absolute certainty only that the segments of branches which are drawn as light curves in the figure are composed of unstable configurations and the segments of the branches ζ and α drawn as heavy curves are composed of stable configurations.

ACKNOWLEDGMENTS

This research was supported by the National Science Foundation under Grant No. DMS-97-05016 and the U. S. Public Health Service under Grant No. GM34809. D.S. acknowledges support from the Program in Mathematics and Molecular Biology at the Florida State University with funding from the Burroughs Wellcome Fund Interfaces Program.

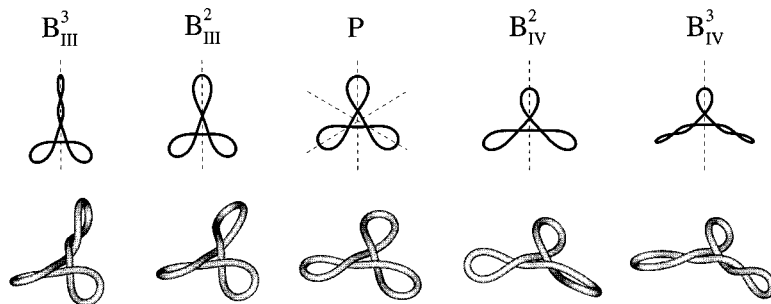
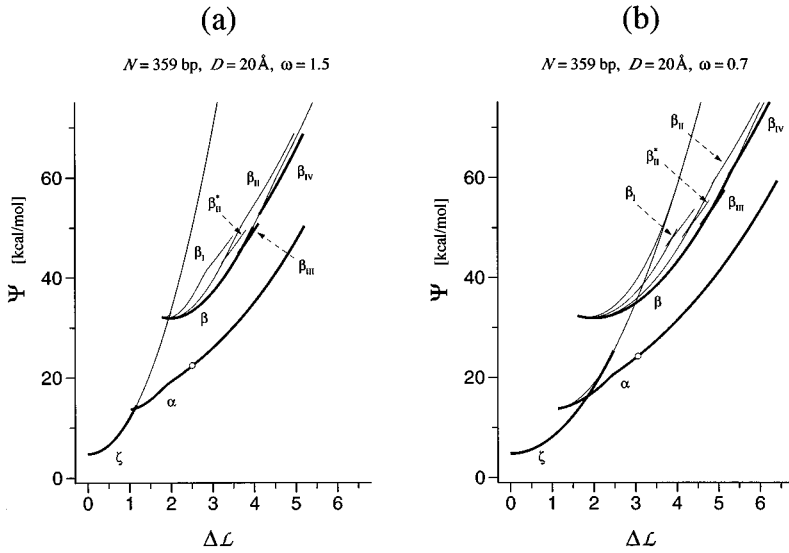


FIG. 11. Selected configurations in branches β_{III} and β_{IV} .

$\Delta\mathcal{L}$	4.000	3.625	3.972	4.124	4.999
\mathcal{W}	3.125	2.771	2.802	3.139	3.861
$\Delta\mathcal{T}$	0.875	0.854	1.170	0.985	1.138
Ψ	49.48	44.95	50.10	52.62	65.62



APPENDIX A: TRANSITIONS BETWEEN CONFIGURATIONS

Figure 12 contains graphs of Ψ versus $\Delta\mathcal{L}$ for fixed values of N and D , and two values of $\omega = C/A$ near the extreme points of the range of ω that has been reported as compatible with experiment. In each case there is a critical value $\Delta\mathcal{L}^c$ of $\Delta\mathcal{L}$ such that each configuration in branch α gives a *global* minimum to Ψ when $\Delta\mathcal{L} > \Delta\mathcal{L}^c$ (at $\omega = 1.5$, $\Delta\mathcal{L}^c = 1.123$; at $\omega = 0.7$, $\Delta\mathcal{L}^c = 1.848$) and there is an interval \mathcal{J} of values of $\Delta\mathcal{L} > \Delta\mathcal{L}^c$ for which there are two configurations that obey the θ condition: $A(\Delta\mathcal{L})$ in α and $B(\Delta\mathcal{L})$ in β .

In this Appendix we discuss matters that can be regarded as extrapolations of results given in the text, and that suggest routes by which one may seek to extend the present theory to the point where it permits treatment of the kinetics of transitions between locally stable configurations. If we assume the validity of the conjecture of sufficiency of the θ condition for stability of equilibrium configurations of plasmids [30], then, for each $\Delta\mathcal{L}$ in \mathcal{J} , the configuration $B(\Delta\mathcal{L})$ gives a local minimum $\Psi(B(\Delta\mathcal{L}))$ to Ψ , and it becomes meaningful to ask questions about the activation energy $\Delta\Psi$ for a transition from $B(\Delta\mathcal{L})$ to $A(\Delta\mathcal{L})$. A familiar ‘‘mountain pass theorem’’ then tells us that, for a given $\Delta\mathcal{L}$ in \mathcal{J} , $\Delta\Psi$ is no less than the

minimum $\Delta\Psi^\#(\Delta\mathcal{L})$ of differences between $\Psi(B(\Delta\mathcal{L}))$ and Ψ at unstable equilibrium configurations with the same $\Delta\mathcal{L}$. We find that, as $\Delta\mathcal{L}$ varies over \mathcal{J} , the maximum value, $\Delta\Psi^\dagger$, of these lower bounds, $\Delta\Psi^\#(\Delta\mathcal{L})$, is attained at $\Delta\mathcal{L} = \Delta\mathcal{L}^\dagger = 3.282$ for $\omega = 1.5$, and at $\Delta\mathcal{L}^\dagger = 4.335$ for $\omega = 0.7$. We here focus our attention on the transitions $B(\Delta\mathcal{L}^\dagger) \rightarrow A(\Delta\mathcal{L}^\dagger)$.

For both $\omega = 1.5$ and $\omega = 0.7$, when $\Delta\mathcal{L} = \Delta\mathcal{L}^\dagger$, there are four unstable equilibrium configurations close to $B(\Delta\mathcal{L}^\dagger)$: one on each of the secondary branches, β_I , β_{II} , and two on the tertiary branch β_{II}^* . These are labeled B_I , B_{II} , $B_{II(1)}^*$, $B_{II(2)}^*$ in Fig. 13. For $\omega = 1.5$ and 0.7 , the lower bound of the height of the energy barriers at $\Delta\mathcal{L}^\dagger$, i.e., $\Delta\Psi^\dagger = \Delta\Psi^\#(\Delta\mathcal{L}^\dagger)$, is attained on two paths, one taking B to A through B_{II} , and the other taking B to A through $B_{II(1)}^*$. (For $\omega = 1.5$, $\Delta\Psi^\dagger = 3.48$ kcal/mol or $5.6 k_B T$ per molecule at $T = 310$ K; for $\omega = 0.7$, $\Delta\Psi^\dagger = 3.29$ kcal/mol or $5.3 k_B T$.) These, as well as transition paths from B to A involving the configurations B_I and $B_{II(2)}^*$, and hence with energy barriers higher than $\Delta\Psi^\#(\Delta\mathcal{L}^\dagger)$ (albeit less than $1/2 k_B T$ higher in the case of the path $B \rightarrow B_{II(2)}^* \rightarrow A$) are depicted in Fig. 14.

The total decrease in Ψ for the transition $B \rightarrow A$ at $\Delta\mathcal{L}^\dagger$ is

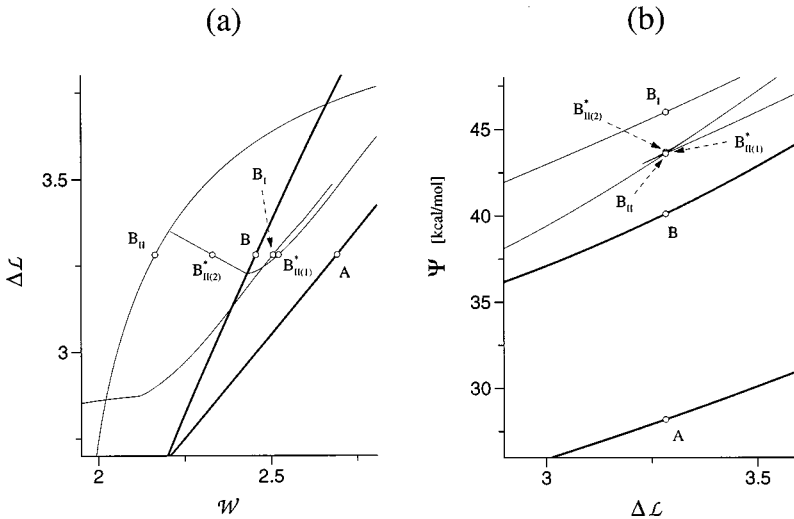


FIG. 13. Graphs of $\Delta\mathcal{L}$ versus \mathcal{W} and Ψ versus $\Delta\mathcal{L}$ for $\omega = 1.5$. The configurations corresponding to points \circ have $\Delta\mathcal{L} = \Delta\mathcal{L}^\dagger = 3.282$ and are shown in Fig. 14. The corresponding graphs for $\omega = 0.7$ have the same structure with, of course, a change in $\Delta\mathcal{L}^\dagger$ and the values of Ψ at B_I , B_{II} , $B_{II(1)}^*$, $B_{II(2)}^*$, and A .

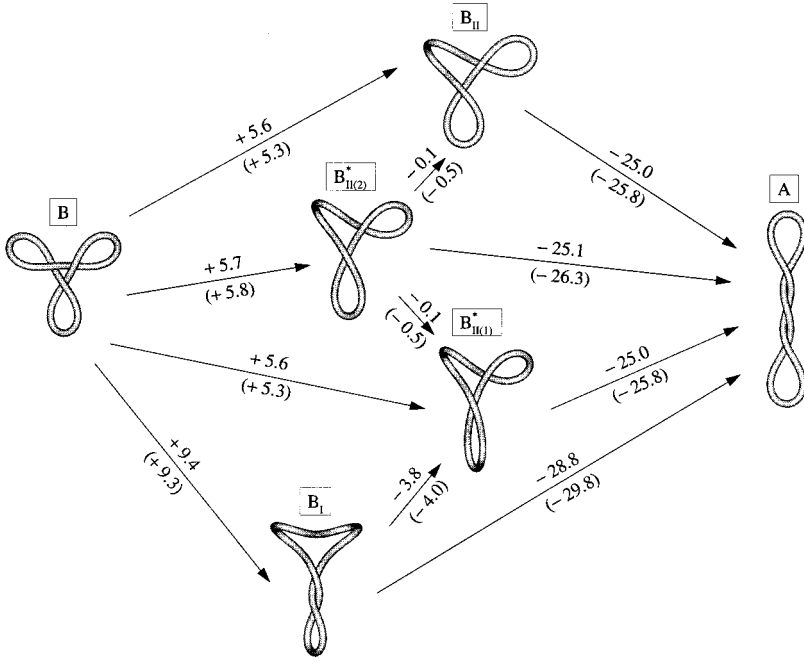


FIG. 14. Transition diagram for configurations with $\omega=1.5$ and $\Delta\mathcal{L}=\Delta\mathcal{L}^\dagger=3.282$. The configuration labeled A is that which minimizes Ψ in the class of configurations with $\Delta\mathcal{L}=\Delta\mathcal{L}^\dagger$, B is a locally stable configuration in β , and B_I , B_{II} , $B_{II(1)}^*$, $B_{II(2)}^*$ are unstable equilibrium configurations. The numbers above the arrows indicating the direction of transitions give the corresponding increments in Ψ (in units of $k_B T$). An analogous diagram holds for $\omega=0.7$, which yields $\Delta\mathcal{L}^\dagger=4.335$, increments in Ψ as shown in parentheses, and configurations B, B_I , B_{II} , $B_{II(1)}^*$, $B_{II(2)}^*$ and A that (with the scale and lines of view employed) are nearly indistinguishable from those shown here.

$19.4 k_B T$ for $\omega=1.5$ and $20.5 k_B T$ for $\omega=0.7$. Our calculation of the configurations $A(\Delta\mathcal{L}^\dagger)$ and their energies for cases in which self-contact occurs in intervals required an extension of the method used elsewhere in the paper. A forthcoming paper will deal with explicit representations of equilibrium configurations with intervals of self-contact.

The calculations summarized in Fig. 14, although given for illustrative purposes only, suggest the following conclusion: although the value $\Delta\mathcal{L}^\dagger$ of $\Delta\mathcal{L}$ that maximizes the lower bound $\Delta\Psi^\#(\Delta\mathcal{L})$ for the activation energy for a transition from the branch β is sensitive to the value of ω , that maximum, $\Delta\Psi^\dagger=\Delta\Psi^\#(\Delta\mathcal{L}^\dagger)$, is not.

APPENDIX B: STABILITY OF CIRCULAR CONFIGURATIONS OF MINIPLASMIDS

The fact that for each specified value of the writhe the bending energy Ψ_B of a miniplasmid is minimized on branch α yields a straightforward proof that an equilibrium configuration $\mathcal{Z}^\#$ in ζ , i.e., with $\mathcal{C}^\#$ a circle, is stable if $0 < \Delta\mathcal{L}(\mathcal{Z}^\#) < \Delta\mathcal{L}^\alpha$, and is unstable if $\Delta\mathcal{L}(\mathcal{Z}^\#) > \Delta\mathcal{L}^\alpha$, where, by Eq. (12), $\Delta\mathcal{L}^\alpha = \omega^{-1}\sqrt{3}$. That proof goes as follows.

According to our definition, an equilibrium configuration $\mathcal{Z}^\#$ of a plasmid is stable if there is a neighborhood of $\mathcal{Z}^\#$ such that for each configuration \mathcal{Z} in that neighborhood that has $\Delta\mathcal{L}$ equal to $\Delta\mathcal{L}(\mathcal{Z}^\#)$ and is not equivalent to $\mathcal{Z}^\#$, there holds $\Psi(\mathcal{Z}) > \Psi(\mathcal{Z}^\#)$. To prove that $\mathcal{Z}^\#$ is unstable, it suffices to show that in each neighborhood of $\mathcal{Z}^\#$ there is a configuration \mathcal{Z}^\dagger with $\Delta\mathcal{L}$ equal to $\Delta\mathcal{L}(\mathcal{Z}^\#)$ and $\Psi(\mathcal{Z}^\dagger) < \Psi(\mathcal{Z}^\#)$.

Let us write $\Delta\mathcal{L}^\#, \Delta\mathcal{T}^\#, \mathcal{W}^\#, \mathcal{C}^\#, \Psi^\#$ etc., for $\Delta\mathcal{L}(\mathcal{Z}^\#)$, $\Delta\mathcal{T}(\mathcal{Z}^\#)$, $\mathcal{W}(\mathcal{Z}^\#)$, $\mathcal{C}(\mathcal{Z}^\#)$, $\Psi(\mathcal{Z}^\#)$, etc. Of course, since $\mathcal{C}^\#$ is a circle, $\mathcal{W}^\#=0$. In the units employed for Ψ_B and Ψ_T in Eqs. (2), the bending energy of a circle is equal to $2\pi^2$; hence $\Psi_B^\#=2\pi^2$. Moreover, the bending energy of a circle is strictly less than the bending energy of all noncircular closed curves. Since $\Delta\Omega$ is independent of s in an equilibrium con-

figuration, Eqs. (2) and (4) yield $\Psi_T^\#=2\pi^2\omega(\Delta\mathcal{T}^\#)^2=2\pi^2\omega(\Delta\mathcal{L}^\#)^2$.

We suppose first that $0 < \Delta\mathcal{L}^\# < \Delta\mathcal{L}^\alpha$. Let \mathcal{Z} be a configuration that is not equivalent to $\mathcal{Z}^\#$ and is in an appropriately chosen neighborhood of $\mathcal{Z}^\#$ with $\Delta\mathcal{L}(\mathcal{Z})=\Delta\mathcal{L}^\#$, and let $\hat{\mathcal{Z}}$ be the equilibrium configuration in branch α with $\mathcal{W}(\hat{\mathcal{Z}})=\mathcal{W}(\mathcal{Z})$, and hence with $\Psi_B(\mathcal{Z}) \geq \Psi_B(\hat{\mathcal{Z}})$. In view of the fact that, of all configurations with a given value of $\Delta\mathcal{T}$, that for which $\Delta\Omega$ is constant minimizes Ψ_T , we have $\Psi_T(\mathcal{Z}) \geq 2\pi^2\omega\Delta\mathcal{T}(\mathcal{Z})^2$ and, by Eqs. (1) and (4),

$$\begin{aligned} \Psi(\mathcal{Z}) - \Psi^\# &= \Psi_T(\mathcal{Z}) - \Psi_T^\# + \Psi_B(\mathcal{Z}) - \Psi_B^\# \\ &\geq -4\pi^2\omega\Delta\mathcal{L}^\#\mathcal{W}(\mathcal{Z}) + \Psi_B(\hat{\mathcal{Z}}) - 2\pi^2 \\ &\quad + O(\mathcal{W}(\mathcal{Z})^2). \end{aligned} \quad (\text{B1})$$

Since $\mathcal{C}(\hat{\mathcal{Z}})$ is a closed curve, $\Psi_B(\hat{\mathcal{Z}}) \geq 2\pi^2$. If $\mathcal{W}(\mathcal{Z}) < 0$, then, because $\Delta\mathcal{L} > 0$, we have $\Psi(\mathcal{Z}) > \Psi^\#$. If $\mathcal{W}(\mathcal{Z}) = 0$, then, we have $\Delta\mathcal{L}(\mathcal{Z}) = \Delta\mathcal{L}^\#$ and $\Delta\mathcal{T}(\mathcal{Z}) = \Delta\mathcal{T}^\#$, and in order for \mathcal{Z} to not be equivalent to $\mathcal{Z}^\#$, it must be the case that $\mathcal{C}(\mathcal{Z})$ is not a circle and $\Psi_B(\mathcal{Z}) > 2\pi^2$, which again yields $\Psi(\mathcal{Z}) > \Psi^\#$. For the remaining possibility, i.e., $\mathcal{W}(\mathcal{Z}) > 0$, we note that as $\mathcal{W}^\#=0$, the neighborhood of $\mathcal{Z}^\#$ in which \mathcal{Z} lies can be chosen so that $\mathcal{W}(\mathcal{Z})$ is small and, by Eqs. (12) and (14) (with $m=2$) and the facts that $\Psi_B(\hat{\mathcal{Z}}) \geq 2\pi^2$ and $\mathcal{W}(\hat{\mathcal{Z}})=\mathcal{W}(\mathcal{Z})$, we have

$$\Psi_B(\hat{\mathcal{Z}}) = 2\pi^2 + 4\pi^2\omega\Delta\mathcal{L}^\alpha\mathcal{W}(\mathcal{Z}) + O(\mathcal{W}(\mathcal{Z})^2), \quad (\text{B2})$$

which, when combined with the relation (B1), yields

$$\Psi(\mathcal{Z}) - \Psi^\# \geq 4\pi^2\omega(\Delta\mathcal{L}^\alpha - \Delta\mathcal{L}^\#)\mathcal{W}(\mathcal{Z}) + O(\mathcal{W}(\mathcal{Z})^2), \quad (\text{B3})$$

and hence shows that, if the neighborhood of $\mathcal{Z}^\#$ is chosen small enough, then $\Psi(\mathcal{Z}) > \Psi^\#$, even if $\mathcal{W}(\mathcal{Z}) > 0$; this completes the proof that $\mathcal{Z}^\#$ is stable when $\Delta\mathcal{L}^\# < \Delta\mathcal{L}^\alpha$.

Suppose now that $\Delta\mathcal{L}^\# > \Delta\mathcal{L}^\alpha$. For each positive number Ψ^\dagger , let $\hat{\mathcal{Z}}$ be the configuration in α with writhe \mathcal{W}^\dagger , and let \mathcal{Z}^\dagger be the configuration with $\mathcal{C}(\mathcal{Z}^\dagger) = \mathcal{C}(\hat{\mathcal{Z}})$ that has $\Delta\Omega$ independent of s and such that $\Delta\mathcal{L}(\mathcal{Z}^\dagger) = \Delta\mathcal{L}^\#$ [i.e., such that $\Delta\mathcal{T}(\mathcal{Z}^\dagger) = \Delta\mathcal{L}^\# - \mathcal{W}^\dagger$]. As $\mathcal{W}^\dagger \rightarrow 0$, the configuration \mathcal{Z}^\dagger approaches $\mathcal{Z}^\#$. By Eq. (2), $\Psi_T(\mathcal{Z}^\dagger) = 2\pi^2\omega(\Delta\mathcal{L}^\# - \mathcal{W}^\dagger)^2$, and the argument that gave us (B2) here yields

$$\Psi_B(\mathcal{Z}^\dagger) = 2\pi^2 + 4\pi^2\omega\Delta\mathcal{L}^\alpha\mathcal{W}^\dagger + O((\mathcal{W}^\dagger)^2). \quad (\text{B4})$$

Hence,

$$\begin{aligned} \Psi(\mathcal{Z}^\dagger) - \Psi^\# &= 2\pi^2(1 + 2\omega\Delta\mathcal{L}^\alpha\mathcal{W}^\dagger + \omega(\Delta\mathcal{L}^\# - \mathcal{W}^\dagger)^2) \\ &\quad - 2\pi^2(1 + \omega(\Delta\mathcal{L}^\#)^2) \\ &= -4\pi^2\omega(\Delta\mathcal{L}^\# - \Delta\mathcal{L}^\alpha)\mathcal{W}^\dagger + O((\mathcal{W}^\dagger)^2). \end{aligned} \quad (\text{B5})$$

Because $\Delta\mathcal{L}^\# > \Delta\mathcal{L}^\alpha$, the right-hand side of Eq. (B4) is negative, i.e., $\Psi(\mathcal{Z}^\dagger) < \Psi^\#$ whenever \mathcal{W}^\dagger is sufficiently small.

-
- [1] I. Tobias, D. Swigon, and B. D. Coleman, preceding paper, *Phys. Rev. E* **61**, 747 (2000).
- [2] M. Le Bret, *Biopolymers* **23**, 1835 (1984).
- [3] F. Jülicher, *Phys. Rev. E* **49**, 2429 (1994).
- [4] I. Tobias, B. D. Coleman, and W. Olson, *J. Chem. Phys.* **101**, 10 990 (1994).
- [5] B. D. Coleman, I. Tobias, and D. Swigon, *J. Chem. Phys.* **103**, 9101 (1995).
- [6] D. Swigon, B. D. Coleman, and I. Tobias, *Biophys. J.* **74**, 2515 (1998).
- [7] G. Calugareanu, *Czechoslovak Math. J.* **11**, 588 (1961).
- [8] J. H. White, *Am. J. Math.* **91**, 693 (1969).
- [9] F. B. Fuller, *Proc. Natl. Acad. Sci. USA* **68**, 815 (1971).
- [10] J. H. White, in *Mathematical Methods for DNA Sequences* (CRC, Boca Raton, Florida, 1989), p. 225.
- [11] D. Swigon, *Configurations with Self-Contact in the Theory of the Elastic Rod Model for DNA* (Rutgers University, NJ, 1999).
- [12] W. F. Pohl, *J. Math. Mech.* **17**, 975 (1968).
- [13] P. J. Hagerman, *Annu. Rev. Biophys. Biophys. Chem.* **17**, 265 (1988).
- [14] D. S. Horowitz and J. C. Wang, *J. Mol. Biol.* **173**, 75 (1984).
- [15] The values of C compatible with the data for miniplasmids reported in Ref. [14] are centered about $\omega = 1.4$, which value was employed in the preceding paper.
- [16] J. M. Schurr, B. S. Fujimoto, P. Wu, and L. Song, in *Topics in Fluorescence Spectroscopy, Vol. 3: Biochemical Applications*, edited by J. R. Lakowicz (Plenum Press, New York, 1992).
- [17] As we remarked in the preceding paper, that the value of C can depend on the method of measurement is a matter of current concern. See, in particular, P. J. Heath, J. B. Clendenning, B. S. Fujimoto, and J. M. Schurr, *J. Mol. Biol.* **260**, 718 (1996).
- [18] J. Shimada and H. Yamakawa, *Biopolymers* **23**, 853 (1984).
- [19] J. Shimada and H. Yamakawa, *J. Mol. Biol.* **184**, 319 (1985).
- [20] M. D. Frank-Kamenetskii, A. V. Lukashin, V. V. Anshelevich, and A. V. Vologodskii, *J. Biomol. Struct. Dyn.* **2**, 1005 (1985).
- [21] J. A. Gebe, S. A. Allison, J. B. Clendenning, and J. M. Schurr, *Biophys. J.* **68**, 619 (1995).
- [22] I. Tobias, *Biophys. J.* **74**, 2545 (1998).
- [23] D. Stigter, *Biopolymers* **16**, 1435 (1977).
- [24] A. Vologodskii and N. Cozzarelli, *Biopolymers* **35**, 289 (1995).
- [25] Linear analyses giving rise to Eq. (12) are familiar in the literature on classical mechanics. For the case $m = 2$ see, e.g., E. E. Zajac, *J. Appl. Mech.* **29**, 136 (1962). For a general dispersion relation for vibrations of twisted rings implying Eq. (12), see B. D. Coleman, M. Lembo, and I. Tobias, *Meccanica* **31**, 565 (1996).
- [26] G. Domokos, *J. Nonlinear Sci.* **5**, 453 (1995).
- [27] Y. Yang, I. Tobias, and W. K. Olson, *J. Chem. Phys.* **98**, 1673 (1993).
- [28] T. P. Westcott, I. Tobias, and W. K. Olson, *J. Chem. Phys.* **107**, 3967 (1997).
- [29] H. Tsuru and M. Wadati, *Biopolymers* **25**, 2083 (1986).
- [30] Our belief in the validity of this assumption, which we employ only for configurations in β , is based on two observations. (i) For a configuration in β obeying the E condition, we have found perturbations that lower Ψ_B at fixed \mathcal{W} only when the θ condition is not obeyed. (ii) Our experience with manipulation of closed elastic rods indicates that, for appropriate $\Delta\mathcal{L}$, configurations in β can withstand gentle perturbations.